ELSEVIER

Journal of Nuclear Materials 266–269 (1999) 1161–1166

journal of nuclear materials

Two-dimensional structure of the detached recombining helium plasma associated with molecular activated recombination

D. Nishijima [a,*], N. Ezumi [a], H. Kojima [a], N. Ohno [a], S. Takamur [a], S.I. Krasheninnikov [b], A.Yu. Pigarov [b]

[a] *Department of Energy Engineering and Science, Graduate School of Engineering, Nagoya University, Furo-cho, Chikusa-ku, Nagoya 464-8603, Japan*

[b] *Plasma Science and Fusion Center, Massachusetts Institute of Technology, Cambridge, MA 02139, USA*

Abstract

The structural change of the detached plasmas associated with the molecular activated recombination (MAR) has been studied in a high density helium plasma with helium or hydrogen puff in the linear divertor plasma simulator, NAGDIS-II. The ion particle flux with the hydrogen gas puff starts to decrease in the upstream region close to the plasma source, compared to that with the helium puff. The reduction of the ion particle flux along the magnetic field is found to depend on the plasma density. With the hydrogen gas puff, the attenuation of the ion particle flux is getting smaller as increasing plasma density, which is opposite tendency in pure helium detached plasma where the conventional electron–ion recombination (EIR) is dominating.

Keywords: Detached plasma; Volume recombination; NAGDIS-II

1. Introduction

Plasma detachment is one of the most important issues of the divertor performance in the magnetically confined fusion devices. Recent experiments on the detached plasma in the tokamaks with a divertor configuration show that a volumetric plasma recombination in the detached plasma plays an important role in the strong decrease of the ion particle flux to the target plate [1–5]. In these devices, a continuum and a series of visible line emissions from highly excited levels due to electron–ion recombination (EIR), which includes radiative and three-body recombinations, have been clearly observed in the detached plasmas, where the electron temperature T_e was estimated from the analysis of these spectra to be about 1 eV [1,2,5].

On the other hand, the importance of molecular activated recombination (MAR) associated with vibrationally excited hydrogen molecules [$H_2(v) + e \rightarrow H^- + H$ followed by $H^- + A^+ \rightarrow H + A$, and $H_2(v) + A^+ \rightarrow AH^+ + H$ followed by $AH^+ + e \rightarrow A + H$, where A^+ (A) is the hydrogen or the impurity ion (atom)] has been theoretically pointed out and discussed [6–10]. The MAR is expected to be a dominating volume recombination process because the rate coefficient of MAR is much larger than that of EIR at $T_e > 0.5$ eV as shown in Fig. 1. We have shown the experimental evidence of the MAR in the helium plasma with the hydrogen gas puff in a linear divertor plasma simulator, NAGDIS-II [11]. The detached plasmas were also analyzed with the 2−D fluid B2 code by taking both EIR and MAR effects into account, which indicates the MAR has strong effect on the structure of the detached plasma [12]. Fig. 2 shows the simulation results on the axial profiles along the magnetic field of the electron density and temperature of the helium plasma with the hydrogen gas puff. With the small amount of hydrogen puff, the structure of the

* Corresponding author. Tel.: +81 52 789 5429; fax: +81 52 789 3944; e-mail: d-nisiji@echo.nuee.nagoya-u.ac.jp.

0022-3115/99/$ – see front matter
PII: S0022-3115(98)00565-0

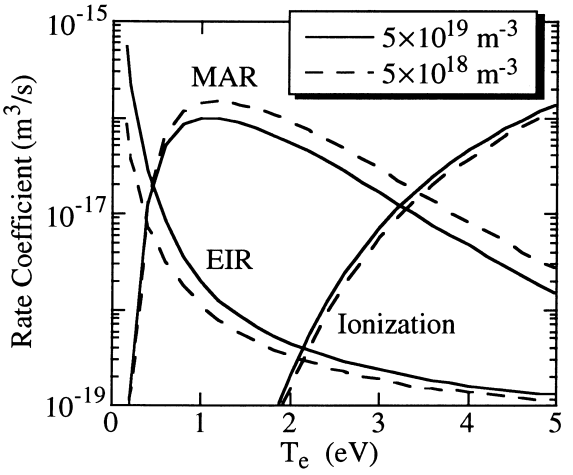

Fig. 1. Rate coefficients of electron–ion recombination (EIR), K_{EIR}, molecular activated recombination (MAR), K_{MAR}, and electron impact ionization of helium atom for helium plasma with molecular hydrogen as a function of electron temperature.

detached plasma is found to be dramatically changed. However, there are no clear experimental investigations on the structural change of the detached plasmas associated with the MAR effects, comparing to the EIR.

In this paper, we will show the spatial profiles of detached helium plasmas with the hydrogen gas puff compared to those with the helium gas puff. The plasma density dependence of the reduction rate of the ion flux along the magnetic field in the pure helium plasma and helium plasma/hydrogen gas mixture is also presented.

2. Experimental setup

The experiments were performed in the linear divertor plasma simulator, NAGDIS-II as shown in Fig. 3 [13]. The length and diameter are 2.5 and 0.18 m, respectively. The magnetic field strength is 0.2 T in the present experiments. Helium is introduced as a primary gas at a pressure of ~1 Torr into the discharge region. High density helium plasmas (electron density $n_e \leqslant 6 \times 10^{19}$ m^{-3}, which is measured by using a double probe measurement) are produced in steady state by the modified TP-D type discharge and flow into the divertor test region through the apertures of the electrically floated intermediate electrode and the anode connected to the ground, whose diameter are 20 and 24 mm, respectively. The plasma column is terminated by the electrically floated target plate, which is made of stainless steel, with a water cooling at the axial position of $X = 2.05$ m from the discharge anode electrode. The divertor plasma test region is equipped with two 2000 l/s turbo molecular pumps, whose pumping speed can be

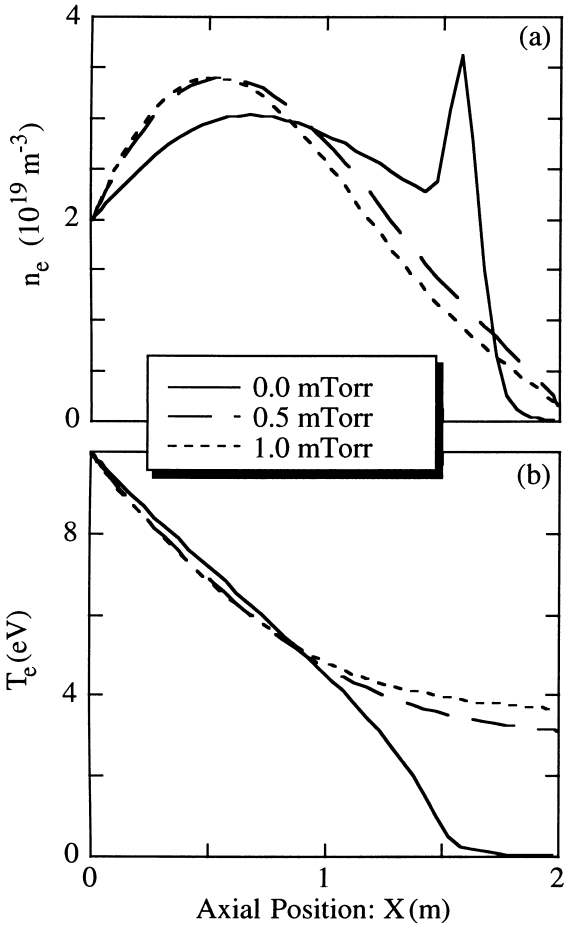

Fig. 2. Typical simulation result on the axial profiles along the magnetic field of: (a) electron density n_e and (b) T_e at the partial pressure of the hydrogen $P_{H_2} \sim 0.0$, 0.5 and 1.0 mTorr, when the plasma parameters at $X \sim 0$ m are: $n_e \sim 2 \times 10^{19}$ m^{-3}, $T_e \sim 10$ eV, ion temperature $T_i \sim 2$ eV and helium gas pressure P_{He} is 10 mTorr.

controlled. The neutral gas pressure P in the divertor test region, measured with a baratron pressure gauge at $X = 1.06$ m, can be controlled from less than 1 mTorr to 30 mTorr by introducing a secondary gas, which is injected near the target plate, into the divertor test region and/or changing the pumping speed. The change of P in the divertor test region has little effect on the plasma production in the discharge region because of three orders of magnitude pressure difference between the discharge region and the divertor test region. Spectra of visible light emissions are detected at two different axial positions of $X = 1.06$ m (upstream) and 1.72 m (downstream). Three sets of fast scanning probes, which provide the radial profiles of plasma column, are also equipped at $X = 1.06$, 1.39 (midstream) and 1.72 m to measure the plasma parameters.

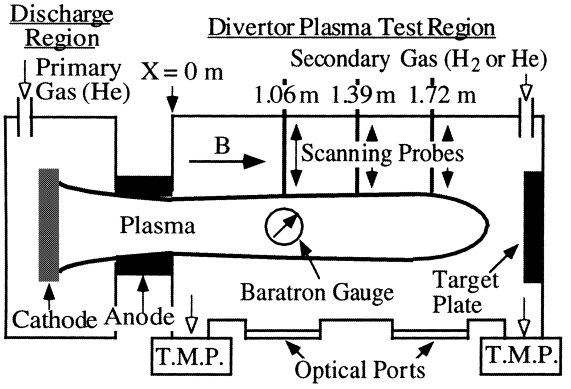

Fig. 3. Schematic of the linear divertor plasma simulator, NAGDIS-II.

3. Experimental results and discussion

3.1. The structural change of the detached plasmas associated with the MAR effects

We generated the helium plasma at a discharge current $I_d \sim 80$ A without any secondary gas puff (initial condition), when the neutral helium gas pressure was kept to be around 4 mTorr using the control of the pumping speed. Fig. 4 shows the spectra of visible light emissions from 310 to 370 nm observed in the downstream ($X = 1.72$ m) in the initial condition and when helium or hydrogen as the secondary gas were introduced. We should notice that the helium or the hydrogen gas puff into the divertor test region had little effect on the plasma production in the discharge region again. As shown in Fig. 4(b), with the helium gas puff of 2 mTorr, the continuum and the series of visible line emissions from highly excited levels, up to the principal quantum number $n \sim 16$, due to the EIR were strongly observed compared to the initial condition in the downstream. On the other hand, in the case of hydrogen gas puff of 2 mTorr in the downstream there was little change in the emission intensity compared to the initial condition as shown in Fig. 4(c). This means the EIR is not enhanced by the hydrogen gas puff, which is different from the case of the helium gas puff. The emissions at 336 nm and 337 nm may be due to NH, which is impurity.

The radial profiles of the ion flux, corresponding to the plasma conditions in Fig. 4, measured in the upstream, midstream and downstream are shown in Fig. 5. When the helium gas was introduced into the plasma with the initial condition, the radial profiles are similar to those in the initial condition both in the upstream and in the midstream. In the downstream, however, the EIR strongly occurs with the helium puff as shown in Fig. 4(b), therefore the ion flux drops. On the other hand, with the hydrogen gas puff the ion flux in the

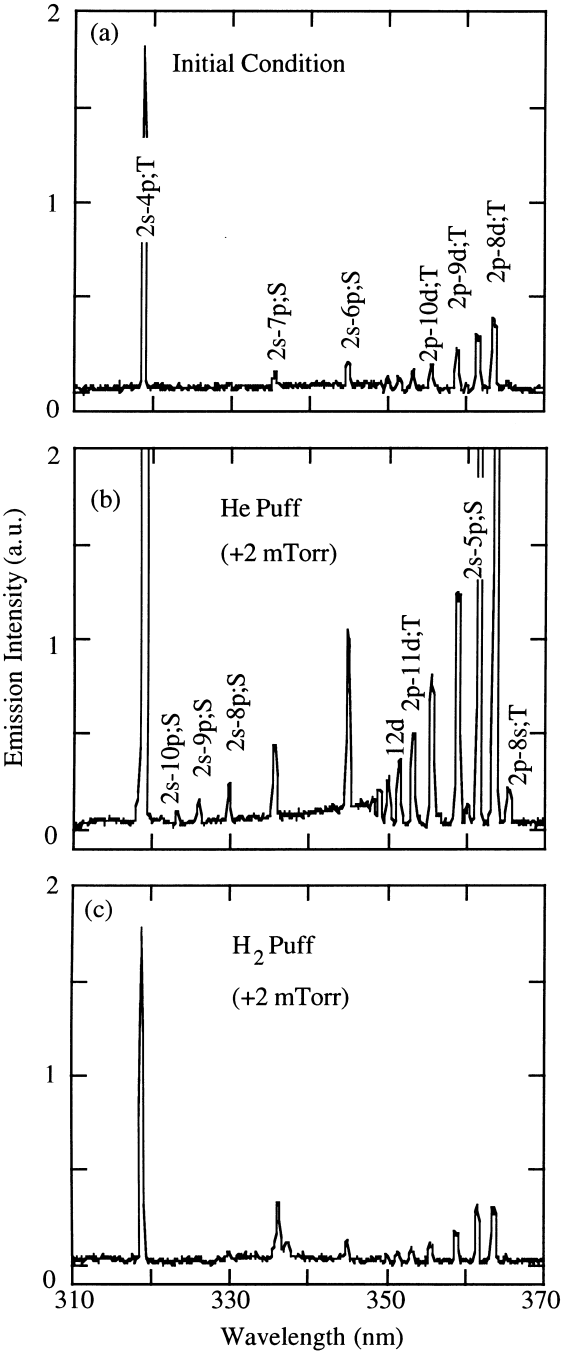

Fig. 4. Emission spectra in the helium plasma at a discharge current $I_d \sim 80$ A in the downstream ($X = 1.72$ m): (a) initial condition; (b) with the helium puff; (c) with the hydrogen puff.

upstream, where T_e is relatively high (around 4 eV obtained with a double probe measurement), already starts to decrease due to the MAR effect compared to that in the case of the pure helium plasmas. Then the ion flux in the helium plasma with the hydrogen gas puff is grad-

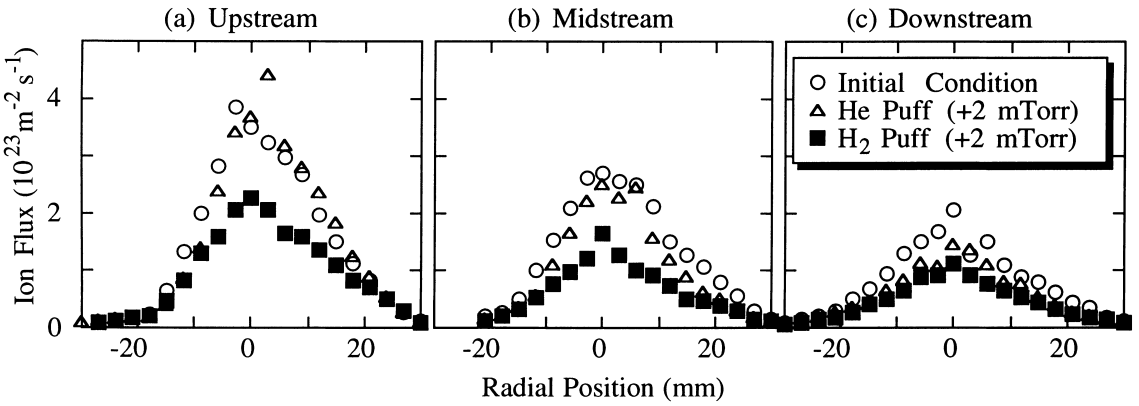

Fig. 5. Radial profiles of the ion flux measured in the upstream ($X = 1.06$ m), midstream ($X = 1.39$ m) and downstream ($X = 1.72$ m) in the same plasma condition as Fig. 4. Open circles and triangles are obtained at $P \sim 4$ mTorr without gas puff and at $P \sim 6$ mTorr with helium gas puff. Closed squares are obtained in the helium plasma with hydrogen gas puff, where the partial pressure of the hydrogen is 2 mTorr.

ually decreasing from the upstream to the downstream, where the EIR does not strongly occur compared to the helium gas puff as shown in Fig. 4(c). Although the ion fluxes in the downstream are almost the same in both cases of the helium and hydrogen gas puff, the gradients of the ion flux along the magnetic field are different. Fig. 6 shows the ratio of Γ_d to Γ_u, where Γ_d and Γ_u are the ion fluxes at the center of the plasma column in the downstream and the upstream, respectively, corresponding to the experimental data in Fig. 5. It is found that the decay length of the ion flux with the hydrogen gas puff is longer than that with the helium gas puff.

These experimental results are in a qualitative agreement with the simulation results predicted by the 2−D fluid B2 code, which takes both EIR and MAR effects in a helium plasma into account [12].

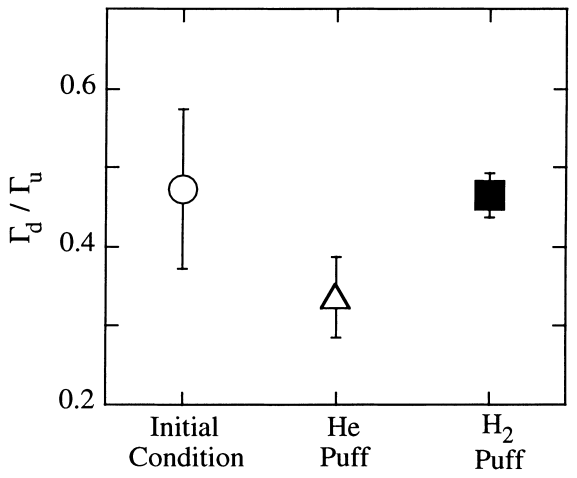

Fig. 6. Ratio of the ion flux in the downstream to upstream, Γ_d/Γ_u, corresponding to Fig. 5.

3.2. Dependence of the ion flux reduction along the magnetic field on the plasma density due to the MAR and EIR

In order to investigate the dependence of the reduction of the ion flux along the magnetic field on the plasma density in the helium plasma with the helium or hydrogen gas puff, we generated the helium plasma with the neutral helium gas pressure of 4 mTorr at $I_d \sim 20$, 50 and 80 A. The plasma densities in the upstream are around 4.0×10^{18}, 1.8×10^{19} and 3.3×10^{19} m^{-3}, respectively. Figs. 7 and 8 show the radial profiles of the ion flux in the upstream and the ratio Γ_d/Γ_u of the ion fluxes in the downstream and the upstream at $I_d \sim 20$, 50 and 80 A in the cases of the helium puff of 2 mTorr and the hydrogen puff of 2 mTorr, respectively. As mentioned above, at any discharge currents, the ion flux of helium plasma/hydrogen gas mixture in the upstream is already smaller than that of pure helium plasma because of the MAR effect. It is found from Fig. 7 that in the case of the helium gas puff, the low density plasma at $I_d \sim 20$ A has a weak reduction of the ion flux from the upstream to the downstream compared to the high density plasma at $I_d \sim 50$ and 80 A. This is because in the low density plasma electrons cannot lose their energy due to electron-ion temperature relaxation process followed by the ion-neutral charge exchange process, because the electron-ion temperature relaxation coefficient is proportional to $n_e^2\ T_e^{-3/2}$, then T_e remains high and moreover the rate coefficient of the EIR, K_{EIR}, is proportional to $n_e\ T_e^{-9/2}$, therefore the EIR cannot strongly occur [14].

On the other hand, in the helium plasma/hydrogen gas mixture, the ratio Γ_d/Γ_u in the low density plasma is smaller than that in the high density plasma as shown in Fig. 8(b). One explanation for this result may be the

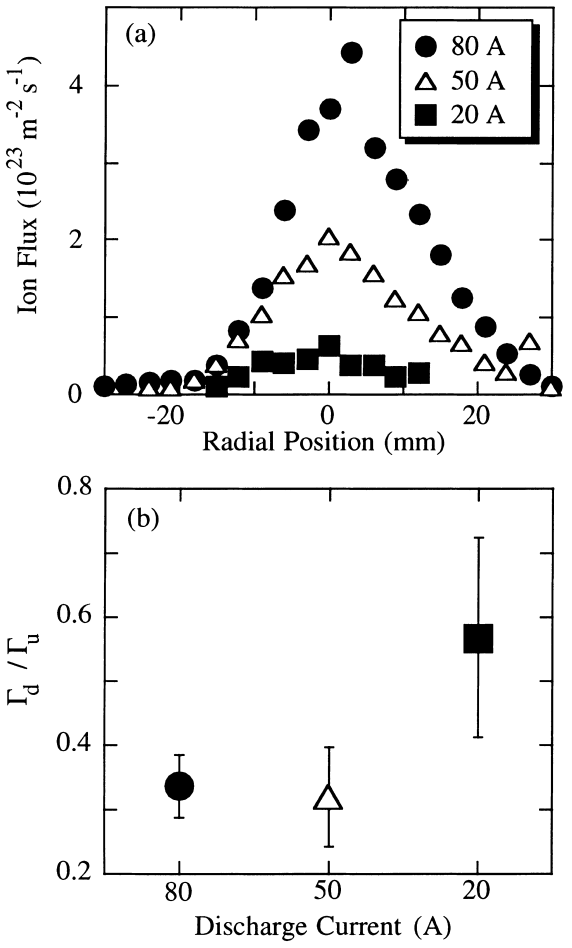

Fig. 7. (a) Radial profiles of the ion flux in the upstream; (b) reduction rate of the ion flux, Γ_d/Γ_u at $I_d \sim 20$, 50 and 80 A with the helium gas puff. Closed squares, open triangles and closed circles are obtained at $I_d \sim 20$, 50 and 80 A, respectively.

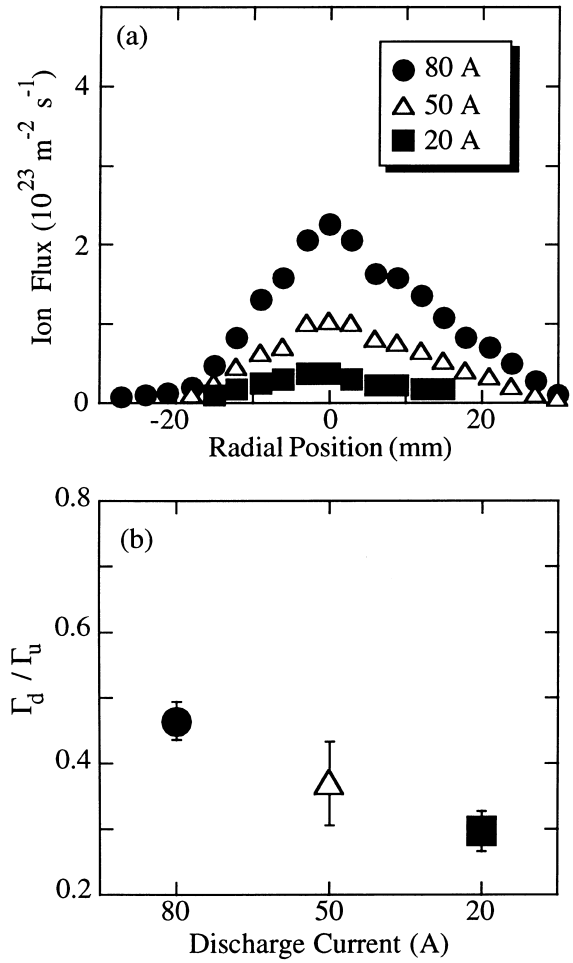

Fig. 8. (a) Radial profiles of the ion flux in the upstream; (b) reduction rate of the ion flux, Γ_d/Γ_u at $I_d \sim 20$, 50 and 80 A with the hydrogen gas puff. Closed squares, open triangles and closed circles are obtained at $I_d \sim 20$, 50 and 80 A, respectively.

difference of the molecular hydrogen density between the low and high density plasmas. The volumetric particle loss rate due to the MAR is proportional to the electron and the molecular hydrogen densities, and is described as $K_{MAR}\, n_e\, n_{H_2}$, where K_{MAR} is the rate coefficient of MAR and n_{H_2} is the molecular hydrogen density. The density of the molecular hydrogen in the high density plasma is thought to become smaller than that in the low density plasma because the attenuation of the molecular hydrogen due to the dissociation and molecular ionization processes is likely to occur in the high density plasma. Furthermore, we must also consider the momentum (pressure) balance in the radial direction [15], which is expected to attenuate the molecular hydrogen influx at room temperature into the plasma due to the energetic hydrogen atom outflux at a few eV generated by the dissociation of hydrogen molecules. Accordingly, the MAR can be more effective in the low density plasma than in the high density plasma. It should also be noted that the rate coefficient of the MAR has an inverse plasma density dependence as shown in Fig. 1.

4. Conclusion

In order to investigate the effect of molecular activated recombination associated with hydrogen molecule on the structure of the detached plasma, we have performed the experiments in the detached helium plasma with the hydrogen gas puff in the linear divertor plasma simulator. We have made a detailed comparison between the hydrogen gas puff and helium gas puff into the helium plasma. Our conclusions are as follows:

(a) With the helium gas puff, electron–ion recombination including radiative and three-body recombi-

nation strongly occurs in the downstream near the target plate, then the ion flux has a steep drop along the magnetic field in the downstream region.
(b) In the case of the hydrogen gas puff, the ion flux gradually decreases over an entire plasma column, when the electron–ion recombination is suppressed compared to the helium gas puff.
(c) With the hydrogen puff, the reduction of the ion particle flux along the magnetic field is getting smaller as increasing in the plasma density, which is opposite tendency in the pure helium detached plasma. This may be associated with the penetration of the hydrogen molecule into the plasma column.

Acknowledgements

The authors wish to thank Dr. Y. Uesugi for discussing the results and Mr. M. Takagi for his technical support in our experiments and Mr. T. Imai and Mr. H. Sawada for their maintenance on the NAGDIS-II.

References

[1] J.L. Terry, B. Lipschultz, A.Yu. Pigarov, S.I. Krasheninnikov, B. LaBombard, D. Lumma, H. Ohkawa, D. Pappas, M. Umansky, Phys. Plasmas 5 (1998) 1759.
[2] D. Lumma, J.L. Terry, B. Lipschultz, Phys. Plasmas 4 (1997) 2555.
[3] G.M. McCracken, M.F. Stamp, R.D. Monk, A.G. Meigs, J. Lingertat, R. Prentice, A. Starling, R.J. Smith, A. Tabasso, Nuclear Fusion 38 (1998) 619.
[4] R.C. Isler, G.R. McKee, N.H. Brooks, W.P. West, M.E. Fenstermacher, R.D. Wood, Phys. Plasmas 4 (1997) 2989.
[5] B. Napiontek, U. Wenzel, K. Behringer, D. Coster, J. Gafert, R. Schneider, A. Thoma, M. Weinlich and ASDEX Upgrade-Team, Proc. of 24th Euro. Phys. Soc. Conf. on Controlled Fusion and Plasma Physics, Berchtesgaden, vol. 21A, Part IV, 1997, pp. 1413–1416.
[6] R.K. Janev, D.E. Post, W.D. Langer, K. Evans, D.B. Heifetz, J.C. Weisheit, J. Nucl. Mater. 121 (1984) 10.
[7] D.E. Post, J. Nucl. Mater. 220–222 (1995) 143.
[8] S.I. Krasheninnikov, A.Yu. Pigarov, D.J. Sigmar, Phys. Lett. A 214 (1996) 285.
[9] A.Yu. Pigarov, S.I. Krasheninnikov, Phys. Lett. A 222 (1996) 251.
[10] S.I. Krasheninnikov, A.Yu. Pigarov, D.A. Knoll, B. LaBombard, B. Lipschultz, D.J. Sigmar, T.K. Soboleva, J.L. Terry, F. Wising, Phys. Plasmas 4 (1997) 1638.
[11] N. Ohno, N. Ezumi, S. Takamura, S.I. Krasheninnikov, A.Yu. Pigarov, Phys. Rev. Lett. 81 (1998) 818.
[12] D. Nishijima, N. Ezumi, K. Aoki, N. Ohno, S. Takamura, Contrib. Plasma Phys. 38 (1998) 55.
[13] N. Ezumi, N. Ohno, Y. Uesugi, J. Park, S. Watanabe, S.A. Cohen, S.I. Krasheninnikov, A.Yu. Pigarov, M. Takagi, S. Takamura, Proc. of 24th Euro. Phys. Soc. Conf. on Controlled Fusion and Plasma Physics, Berchtesgaden, vol. 21A, Part III, 1997, pp. 1225–1228.
[14] N. Ezumi, S. Mori, N. Ohno, M. Takagi, S. Takamura, H. Suzuki, J. Park, J. Nucl. Mater. 241–243 (1997) 349.
[15] S.J. Fielding, P.C. Johnson, D. Guilhem, J. Nucl. Mater. 128–129 (1984) 390.